

¹Murugaanandam S²K. Ramash Kumar³Vishnu Kumar Kaliappan⁴Sabari L Uma Maheswari⁵Rajendrakumar R⁶S. Balakumar

Artificial Neural Network based MPPT Controller with Boost Converter for Varying Solar Insolation in Arba Minch



Abstract: - Solar energy is an elixir of energy that can be used to generate electricity with the help of technology. Ethiopia has an abundance of natural geometric to generate electrical energy from solar irradiation. Renewable energy is a promising word for making the country free of fossil fuels. However, due to low efficiency, it necessitates a variety of methods to maximise output efficiency. In this effort, a MATLAB-SIMULINK PV module model was created to stuff Maximum Power Point (MPP) from solar energy. To test the performance of the proposed model, a closed loop system was created using a conventional controller and an artificial neural network (ANN). The developed model was put through its paces with various isolations. In response to uncertain solar irradiation conditions, the Artificial Neural Network ANN associated with the PV module delivered fast response and minimal oscillations.

Keywords: Artificial neural network (ANN), Maximum power point tracking (MPPT), MATLAB-Simulink, PV(Photo voltaic) module, Solar Irradiation, PV syst, Diverse solar insolation.

I.INTRODUCTION

Because of its environmental benefits, long-term viability, and lack of fuel costs, solar radiation is one of the most promising renewable energy sources. As a result, the number of studies and applications involving PV systems is increasing. PV modules (solar photovoltaic modules) are semiconductor arrangements that convert solar radiation into electricity. PV systems have been deployed in a variety of applications, including communications satellites, cellular technologies, water pumps, electric vehicle applications, and solar power plants. According to the obtained energy values, the proposed PV model has a variation of 3.25 percent for monocrystalline silicon PV panels, 3.70 percent for thin-film panels, and 13.93 percent for polycrystalline silicon panels. The results show that the proposed model generates results that are very close to reality for monocrystalline silicon and thin-film PV panels [1]. A neural network is used in this method to specify the maximum power point reference voltage under various atmospheric conditions. By properly managing the dc-dc boost converter, the maximum power point can be tracked. To validate theory analysis, simulation results are generated using MATLAB/Simulink [2]. This study successfully implemented the design, modelling, and simulation of a fuzzy logic loop driven DC-DC converter with grid linked wind generator in MATLAB/Simulink. In this study, the Inductor-Capacitor Inductor (LCL) type DC-DC resonant converter dominated in terms of reduced EMI effect, stresses, and high power density. The simulated results of the developed controller with system revealed successful tracking of maximum power from the wind at all wind velocities, as well as good load voltage regulation of the converter [3], in comparison to a Proportional integrate

² *Corresponding author: Department of Electrical and Electronics Engineering, Dr.N.G.P.Institute of Technology, Coimbatore-48, Tamilnadu, India. Email: ramash1210@yahoo.co.in

¹ Associate Professor, Department of Networking and Communications, SOC, SRMIST, Kattankullathur 603203. Email: murugaas@srmist.edu.in

³ Professor, Department of Computer Science and Engineering, KPR Institute of Engineering and Technology, Coimbatore, India. Email: vishnukumar.k@kpriet.ac.in

⁴ Assistant professor, R. M. K Engineering College, Tamilnadu, India. Email : slu.eee@rmkec.ac.in

⁵ Assistant Trainer, Electrical Section, Engineering Department, College of Engineering & Technology, University of Technology and Applied Sciences - Shinas, Sultanate of Oman. Email: rajendrakumar.ramadass@utas.edu.om

⁶ Faculty of Electrical and Computer Engineering, Arba Minch University, Arba Minch-21, Ethiopia. Email: sbk25dec@gmail.com

controller (PI) controller. In this paper, deep learning is used to fully learn the latent temporal dependencies from post-disturbance system dynamic trajectories in order to assess short-term voltage stability (STVS) in power systems. The results of the IEEE 39-bus system tests show that the proposed method accurately and timely assesses the system's stability status. The proposed method also outperformed more traditional shallow learning-based assessment techniques [4]. In this study, pattern recognition algorithms were used to identify various distilled spirits brands principal component analysis and the artificial neural network (ANN). Algorithms were compared in terms of their recognition rates. The recognition rates of algorithms were compared. The Back Propagation Neural Network (BPNN) can be used to improve recognition [5]. Microgrids have emerged as a viable alternative to traditional power plants for addressing environmental pollution and energy crises. Coordination of demand response and renewable generation is a critical and difficult problem when it comes to micro grid scheduling. In this study, the Jaya algorithm and the interior point method (IPM) are combined to create a hybrid analysis-heuristic solution method called Jaya-IPM, in which the IPM and the Jaya address the lower and upper levels of the model, and the scheduling scheme is obtained through iterations between the two levels [6]. The proposal generates high-quality renewable scenarios and outperforms current centralised methods in terms of quality and efficiency, according to simulations. The robustness of our method will also be tested in an experiment involving multiple federated learning settings [7]. The researchers learned a lot about PV modules, control strategies, converter topologies, and expert systems from the various research articles. The primary goal of the work is to maximise the power point of solar PV. In this paper, ANN was used in a closed loop to reduce system errors.

II.STATEMENT OF PROBLEMS

Renewable energy resources are plentiful in Ethiopia and can meet the country's goal of complete electrification. In spite of the country's vast energy resources, the sector remains in its early stages. It is estimated that over 80% of Ethiopians live in rural areas without access to modern energy sources and are therefore reliant on traditional biomass fuels [8-9]. The federal government of ethiopia under program 2.0, 2019 targeted to provide electricity to all isolated community populations. The rural electrification have been successfully developed standalone PV power supply to village populations. The existing systems used in the rural electrifications are not equipped with advanced MPPT controllers. This work aims to bring newly developed MPPT controller which will be enhance the operation of PV systems in and out of the rural areas. Ethiopia's renewable energy sector will grow faster as a result of this new paradiam attempt.

III.METEOROLOGICAL DATA OF ETHIOPIA

Table 1. Arba Minch irradiation data by PV system software

Months	Global Horizontal Irradiation Kwh/m ² /month	Horizontal Diffuse Irradiation Kwh/m ² /month	Temperature (°C)	Wind Velocity m/s	Relative Humidity %
January	215.3	43.5	26	3.20	40.1
February	199.2	41.6	27.3	3.40	36.9
March	218.9	56.4	26.5	3.10	49.7
April	210.4	58.4	23.6	2.49	75.2
May	203.0	60.2	23.1	3.00	73.8
June	172.4	69.9	22.3	3.60	65.6
July	164.7	72.4	22.5	3.90	58.6
August	169.1	71.4	22.8	4.00	56.5
September	179.1	67.2	23.6	3.80	55.0
October	198.4	62.8	23.4	3.00	68.9
November	196.2	48.9	22.4	2.59	77.2
December	203.9	44.2	24.1	2.89	55.1

PV current increases slightly as temperature rises, but the PV open-circuit voltage (V_{oc}) drops dramatically, as illustrated in Figure.2. The solar panel's output voltage drops precipitously when the temperature is changed by $45^{\circ}c$, $25^{\circ}c$, or $5^{\circ}c$. If an MPPT controller is developed using advanced techniques to extract maximum power from a solar panel. In order to keep track of the voltage, the MPPT controller compares the measured voltage to a reference voltage. The duty cycle of the boost converter is determined by the controller's results. To determine the range of the reference voltage, the panel's output voltage must have experienced a few fluctuations. Because of this, it is simple to set the reference voltage to track the maximum power output from the panel.

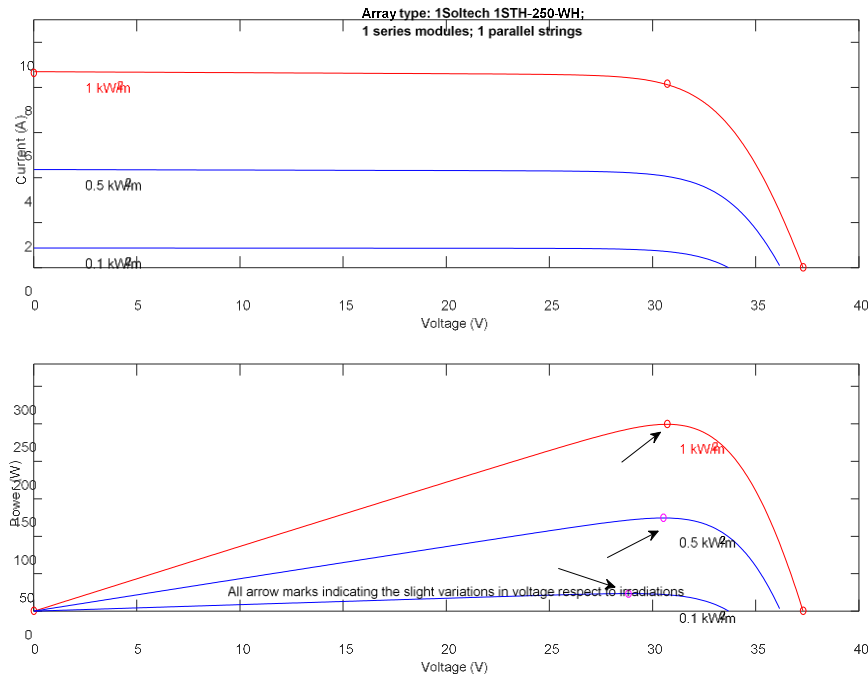


Figure 3. Simulated Responses of Constant Temperature with Different Solar Irradiations

Maintaining a constant temperature of $25^{\circ}c$ and varying the solar irradiation by $1000Kw/m^2$, $500 Kw/m^2$ and $100 Kw/m^2$ can minimize voltage fluctuations. Figure 3 shows that the voltage is nearly constant at a variation in solar insolation. In this paper, we've resolved to be using solar irradiation and temperature as input parameters for ANN.

V.MATHEMATICAL MODELLING APPROACH OF PV (PHOTO VOLTAIC) ARRAY.

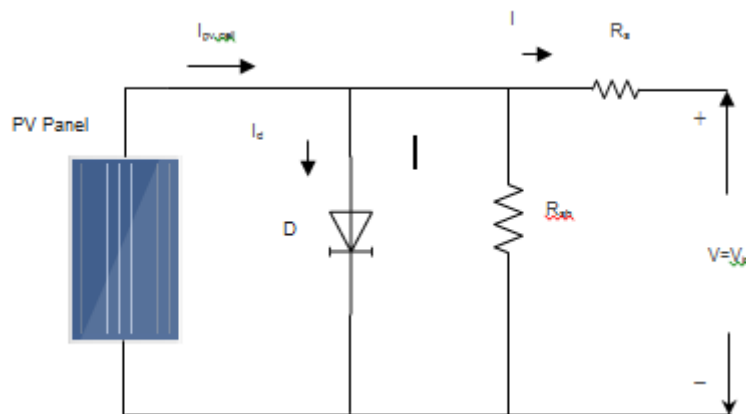


Figure 4. Equivalent Circuit of PV Module

The simplest schematic used in the PV model is shown in Figure 4. It is based on voltage that PV current is computed here. Irradiance and temperature are inputs to the proposed model, while PV current, voltage, and power are outputs. A PV cell's output current (I_o) is directly related to its output voltage (V_o). The following mathematical equations are used to model PV modules. For this photovoltaic system, the manufacturers' module data sheets were consulted. the photo current (I_p) directly proportional to insolation in Kw/m². The band gap energy has increased as a result of the rise in temperature, resulting in an increase in photocurrent. Short circuit current (I_{sc}) and photocurrent (I_p) are nearly equal in magnitude. Temperature increases have led to an increase in short circuits.

In general, short circuit current (I_{sc}) variation was only 0.1 percent per kelvin lower than expected.

$$V_{oc} = nV_T \ln(i_p + i_o / i_o), \tag{1}$$

Here V_T and I_o are the function of the temperature. The I_o is the exponential variation of the temperature. The V_{oc} is inversely proportional to temperature when I_o and V_T are taken into account.

$$V_{oc} = nV_T \ln(i_p / i_o) \tag{2}$$

The reverse saturation current of I_o can be given as

$$i_o \propto T^m e^{-\frac{V_{go}}{nV_T}} \tag{3}$$

$$\frac{dV_{oc}}{dt} = V_{oc} - (V_{go} + mnV_T / T) \tag{4}$$

Traditional value of silicon has $m=1.5$, $n = 2$, $V_T = 0.26V$ at 300 Kelvin temperature, $V_{oc}=0.6V$, we get the value of $-2.1mv/^{\circ}K$. Every PV cell's variation in V_{oc} with temperature is shown here. V_{oc} drops nearly $(-2.1mv/^{\circ}K)$ degrees with a one-degree increase in temperature. The equation (4) was obtained from the analysis of PV equivalent circuit shown in figure.4.

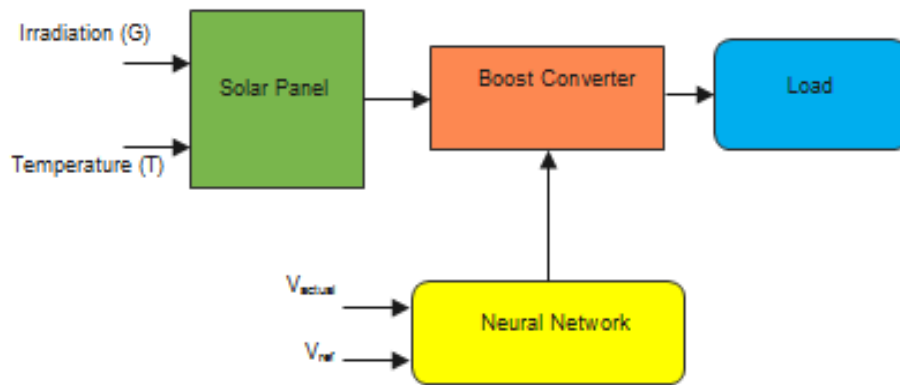


Figure 5. Block diagram of Proposed System

The coefficient kr varies for each PV technology. In this study, kr is taken as 1.509 for monocrystalline, as 1.468 for polycrystalline, and as 1.450 for thin-film technology. Figure 5 depicts the proposed PV model's Simulink block diagram. By taking into account solar radiation and the surrounding temperature, a cell temperature block in PV model Simulink is used to calculate cell temperatures (11).

According to the manufacturer's data and standard test conditions ($G_S = 1000 \text{ W/m}^2$ and $T_S = 25^{\circ}C$), I_{sc} , I_{MP} , V_{OC} , and V_{MP} are the values given in the manufacturer's data sheet, G and T_C are the radiation and cell temperature, respectively. Alpha(α) and beta (β) show the current temperature coefficient and voltage temperature coefficient, respectively.

$$I_o = I_{sc} (1 - Z_1 [e^{(V_o / [Z_2 \cdot V_{oc}])} - 1]) \tag{5}$$

PV cell output current (I_o) is a function of PV output voltage (V_o). PV modules are modelled using the following mathematical equations (5 to 11).

$$Z_1 = (1 - I_{MP} I_{sc}) \cdot e^{(-V_{MP} / (k_2 \cdot V_{oc}))} \tag{6}$$

$$Z_2 = ((V_{MP}/V_{OC}) - 1) \ln (1 - (I_{MP}/I_{SC})) \tag{7}$$

It is seen from (7) that K_1 and K_2 coefficient change according to different PV panel parameters. Variation of these parameters according to the irradiance or cell temperature is given below [1, 10]:

$$I_{SC}(G, T_c) = I_{SC} \cdot G \cdot G_s (1 + \alpha (T_c - T_s)) \tag{8}$$

$$I_{mp}(G, T_c) = I_{mp} \cdot G \cdot (1 + (T_c - T_s)) \tag{9}$$

$$V_{oc}(T_c) = V_{oc} + \beta (T_c - T_s) \tag{10}$$

$$V_{mp}(T_c) = V_{mp} + \beta (T_c - T_s) \tag{11}$$

VI. SIMULINK MODULE

a. PI based MPPT Control

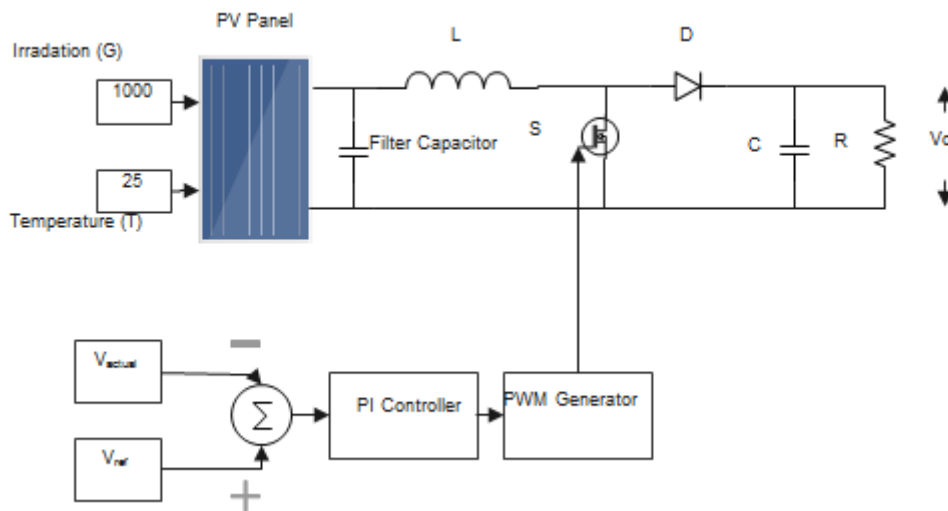


Figure 6. Simulink model of PI based MPPT Control

This model was created to evaluate the efficiency of ANN-MPPT control. The irradiances of the sun change with the passage of time. The sun's irradiance rises in the morning at 6 a.m. and decline in the evening at 5 p.m. The standard insolation to generate power from solar energy is 1Kwh/m² at 25⁰C. In fig.6 shows the modelling of MPPT with PI controller. In this effort, researchers were aimed to model Simulink in MATLAB/Simulink for both ANN-MPPT and PI controller-MPPT.

The varying quantities of sun irradiance were estimated based on Ethiopian irradiance data. In the fig.3 characteristics of solar panel shows that when irradiance had varied from 1Kwh/m², 0.5 Kwh/m², 0.1 Kwh/m² the respective voltages on the curve changes between 29V to 31V. This curve has given the tracking point of the maximum power to extract maximum power from the designed model. In this work, the reference voltage (V_{Ref}) taken as 30V. The proposed controllers have been used to produce the minimum errors by comparing the actual and reference values. In case of PI controller, the proportional value (K_p) and integrate value (K_i) were selected by trail and error method. Initially, the K_p value assumed to be zero and K_i values almost 1.039 to see the system response. The tuned response and block response of system was incoherence lately response of the system was corrected by choosing optimal K_p and K_i values. The boost converter parameters like Inductor (L) and Capacitor (C) values are taken as 0.0073H and 1.9300×10^{-4} F respectively. The output voltage of stepping up converter is 60V. The switching frequency of the stepping-up converter used as 10000 Hz. Fig. 7 show the simulated output and reference power of the stepping up converter. From these results, it is found that the measured power is closely track the reference value with classical PI controller.

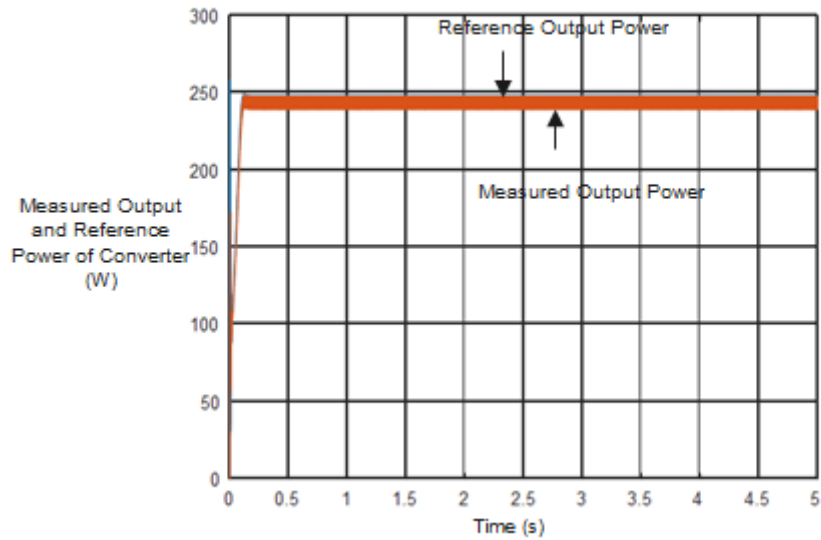


Figure 7. Simulated responses of measured and reference output power of stepping up converter using PI controller

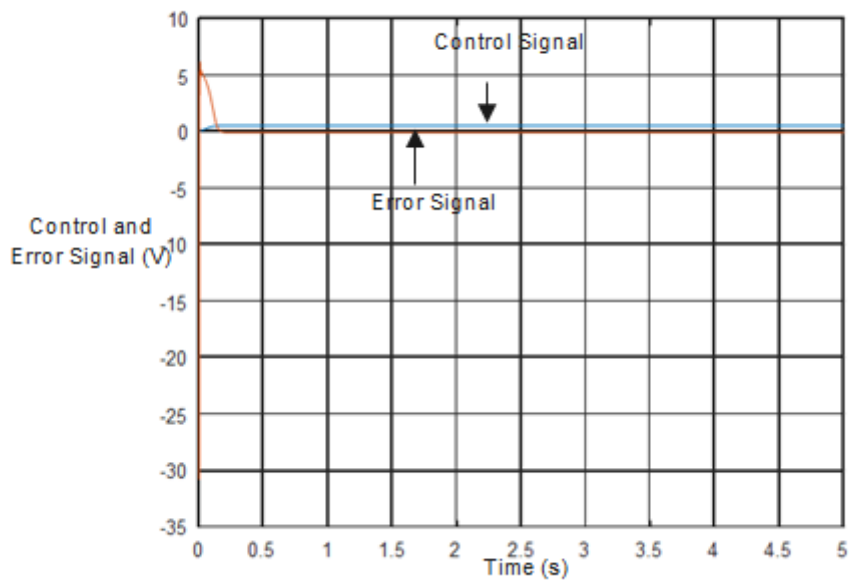


Figure 8. Simulated results of control and error signal of the PI controller

Fig. 8 shows the simulated control and error signal of the PI controller for proposed system. Fig. 9 shows the simulated boost converter and PV output voltage or input voltage of boost converter with PI controller. It evident that the simulated results is very close to theoretical value, zero peak overshoots and quick setting time (transient state) with PI controller.

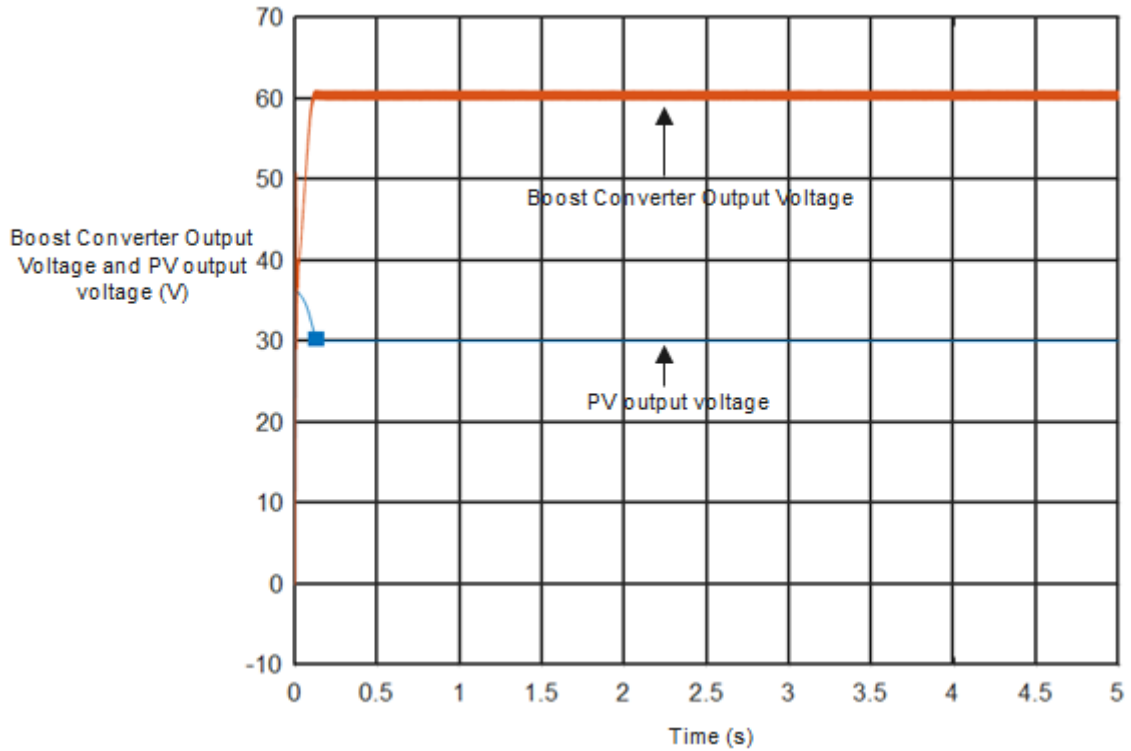


Figure 9. Simulated output voltage of boost converter and PV output voltage with PI controller

b. ANN based MPPT controller

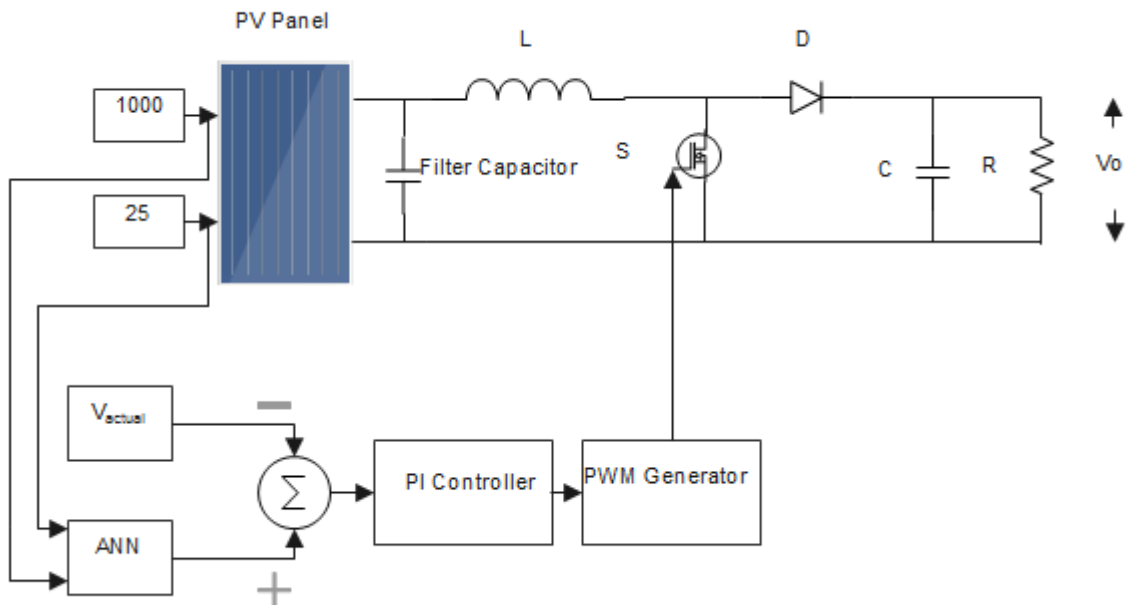


Figure 10. Simulink Model of ANN based PV Module

In this case, the ANN model was fed data on irradiance and temperature. By using an ANN design, the PV panel voltage would remain constant and error would be reduced. Therefore, it was possible to monitor the panel's maximum output power. It was compared to a constant reference voltage that had been measured from the solar panel (refer Figure. 10). The duty cycle of the boost converter would be determined by the PI and ANN

controller's reduced error. In MATLAB 2016, the M-script coding of ANN was developed. Here is the ANN's program for proposed model is recorded in Appendix section (Refer Appendix-I). Figure 10a depicts the proposed ANN controller's flowchart. The irradiance (G) and temperature (T) data were used as input for the model. The total number of data (M) was checked, and it was found to be less than the current number of iterations (N). If the condition is no, train an ANN network with G, T, and V_{mp} . If not, calculate the maximum voltage (V_{mp}) directly and increase the iteration count (N). The figure.10b shows the regression plot of ANN. The Leven berg-Marquardt algorithm was used to train the network to match the input and target. The training network's clear evidence was a regression value(R) close to 1.

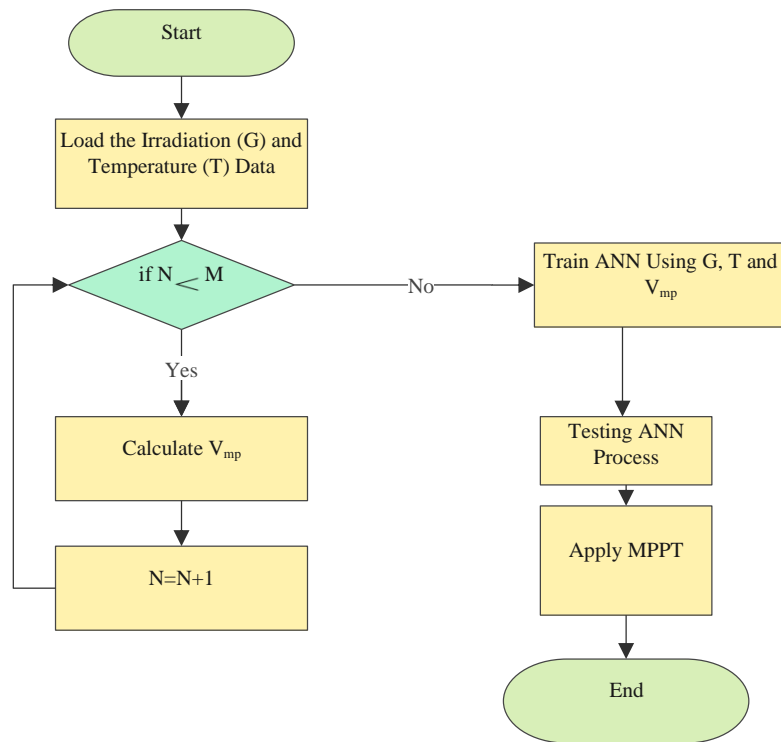


Figure 10a. Flowchart of proposed system with ANN controller

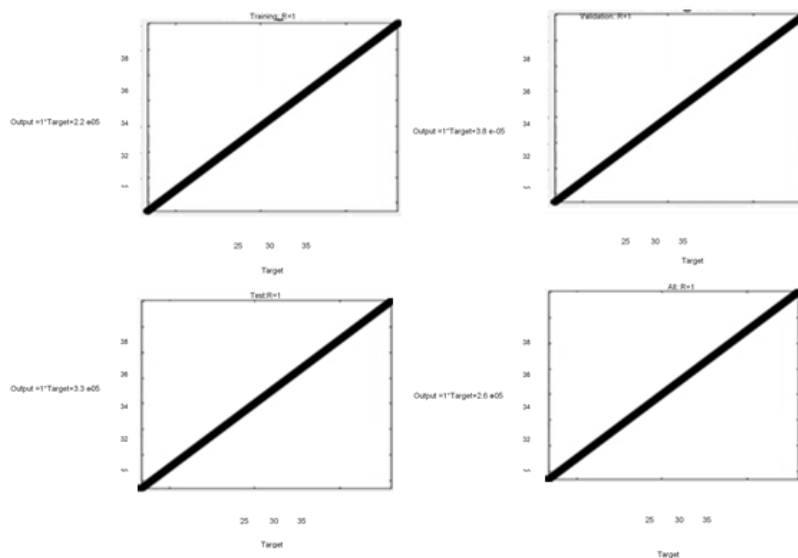


Figure 10b. Regression plot of ANN

Table 2. Parameters of Modelling

S.No	Parameter Name	Values
1	Module	1Soltech 1STH-250WH
2	P_{max}	250.205
3	Cell per module	60
4	V_{oc}	37.3V
5	V_{max}	30.7V
6	V_{Ref}	30V
7	I_{sc}	8.66A
8	I_{max}	8.15A
9	Irradiances (W/m^2)	1000, 500, 100
10	R_{sh}	224.1886 Ω
11	R_s	0.23724 Ω
Control Parameters		
12	Proportional value(P)	0.00011
13	Integral (I)	1.03980769012097
14	Stop time of tune parameter	3
15	On set lag	1.5
16	Sample time	0.1
17	Off set time	0.2
18	Signal time	Step with 0.2 amplitude

VII.RESULTS AND DISCUSSION

The various irradiation conditions were studied in the modelling of artificial neural network-based MPPT and PI controllers. The following section includes waveforms that illustrate how well the Simulink results were observed. In this endeavour, a boost converter was used to increase the solar panel's output. Two controllers were used to form the feedback loop, one of which was a PI controller and the other an ANN. Finally, both controllers aim to minimize error in order to maximize solar panel output. In response to feedback from the controllers, the boost converter's duty cycle was tweaked to fit the new signal.

Fig. 13 show the simulated output and reference power or PV output power of the stepping up converter with ANN. Fig. 14 show the simulated control and error signal of the ANN for proposed system. It evident that the simulated results have proficient time domain specifications using ANN.

Figure 15 shows the overshoot beginning with a PI controller and continuing throughout. In comparison to expectations, the output power was a little lower than expected.

Figures 16 and 17 shows an output voltage of about 48 volts with overshoot and a panel voltage of about 29 volts, respectively. Nearly 25 watts were lost at the converter output side as a result of the voltage fluctuation. This major flaw was eliminated kudos to the ANN controller. The ANN's testing and validation was not completed until it had a correlation (R) of 1 (the highest possible value). Solar panel output current and voltage are depicted in Figures 11 and 12. The solar panel current was nearly 8A and the boost converter current was nearly 4A. Both devices produced 30V and 60V of voltage. As expected, the output power of the boost converter was exactly 250Watts because the output current from the boost converter was nearly less than the output of the PV. In both cases, the goal is to get the most power possible out of the boost converter through the work. However, compared to the boost converter with an ANN controller, the PI controller offered slightly worse performance. In the PI controller modelling, there was a constant loss of 25 Watts. With the help of an ANN controller network, the initial shoot-through was reduced.

There are always some caveats to any scientific finding. Even a small setback can spark new approaches to a research work. This work has limitations in the implementation of practical ANN closed-loop systems. The limitation of the present work will be achieved in future works.

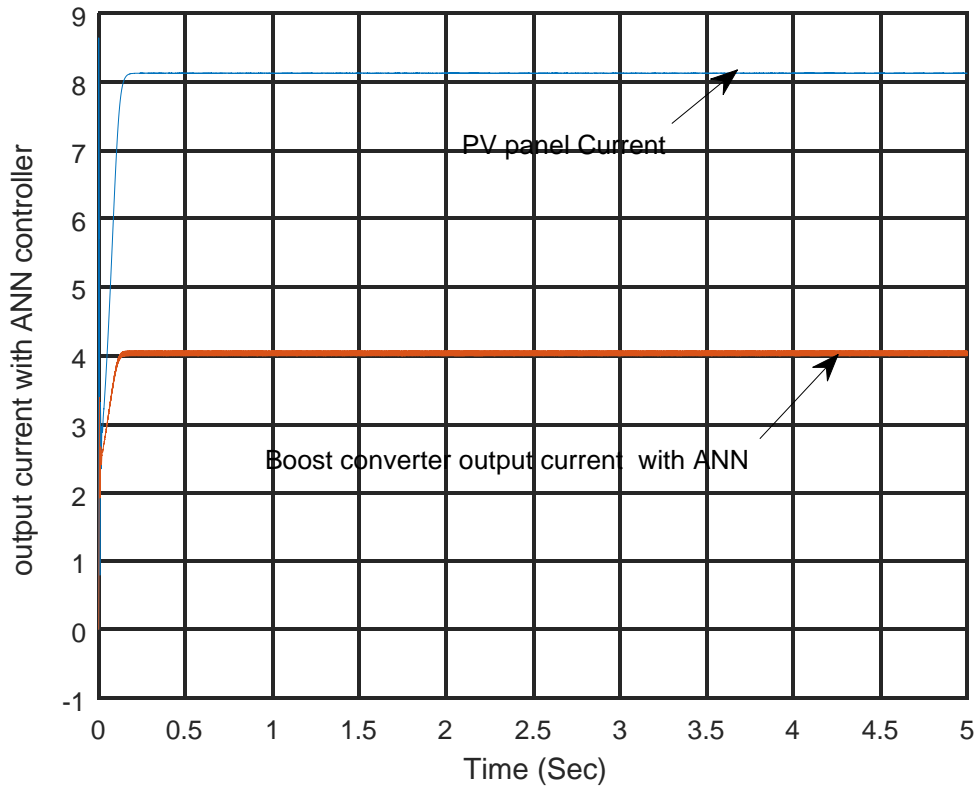


Figure 11. Output current of PV model and converter with ANN controller

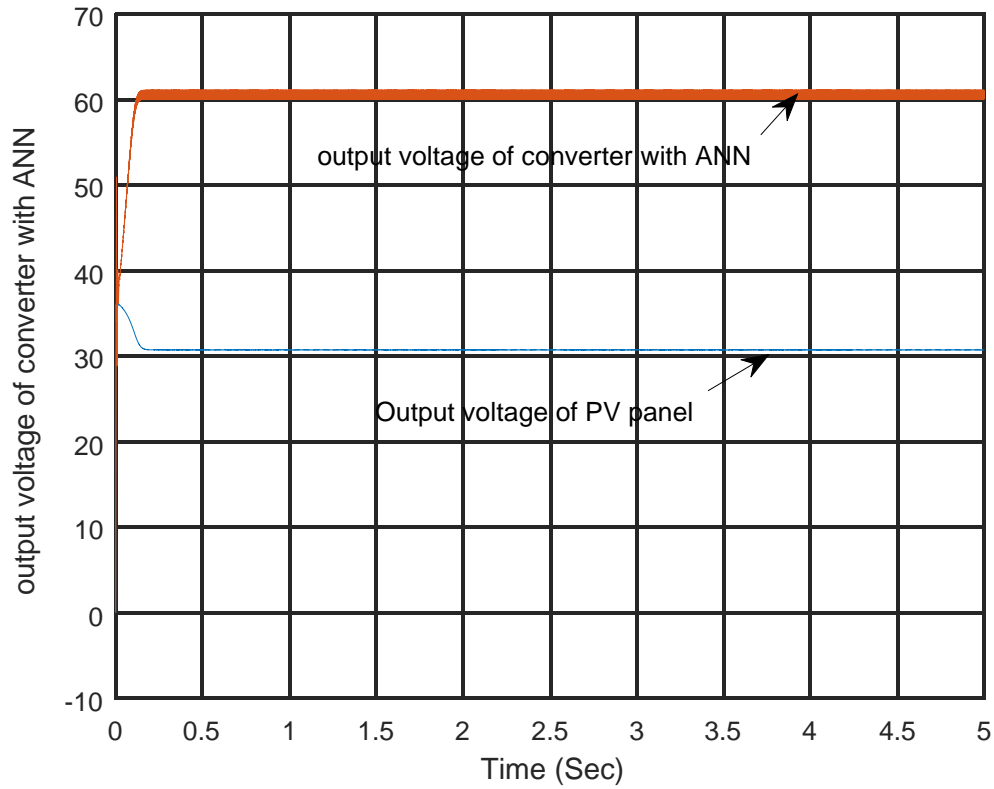


Figure 12. Output Voltage of PV model and converter with ANN controller

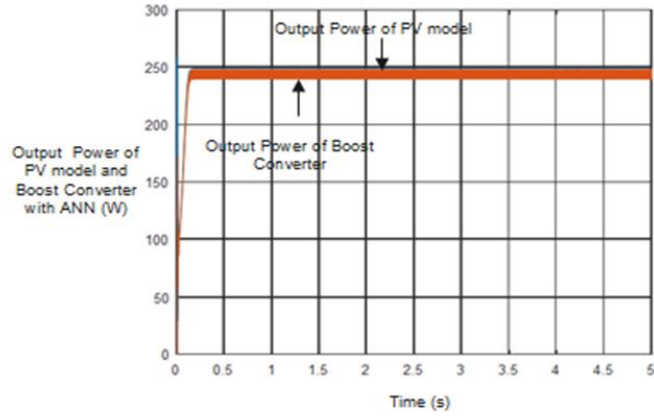


Figure 13. Output power of PV model and converter with ANN controller

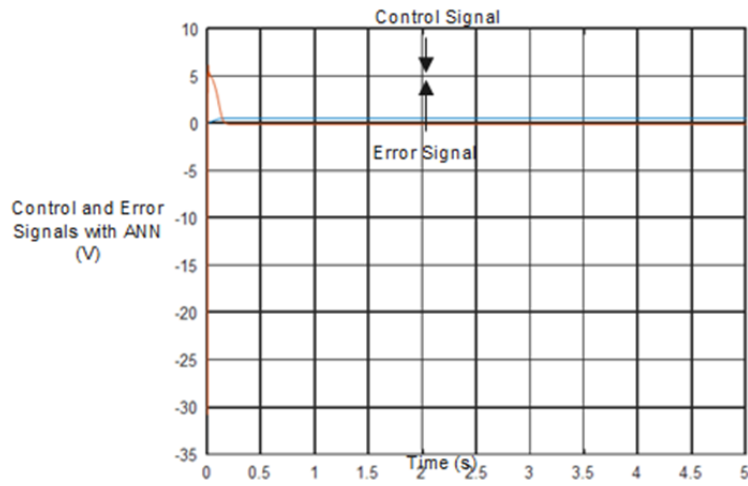


Figure 14. Reference signals of ANN controller

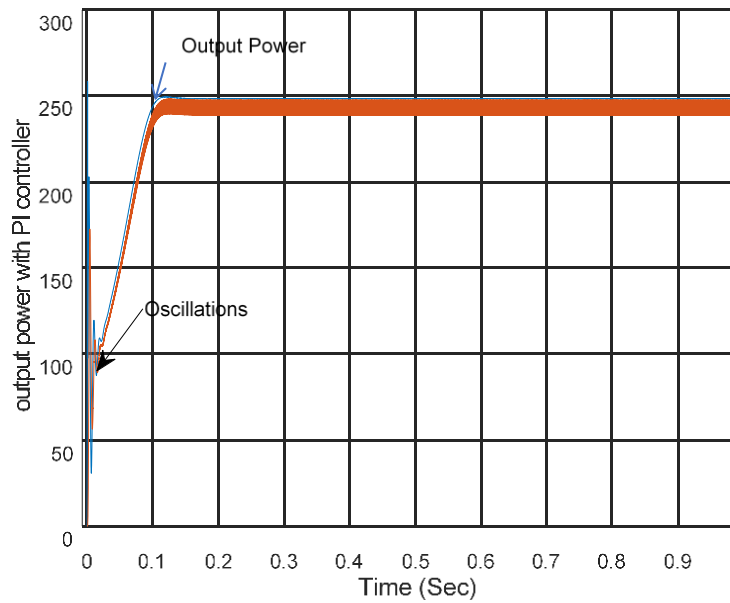


Figure 15. Output power with shoot through with PI controller in transient state

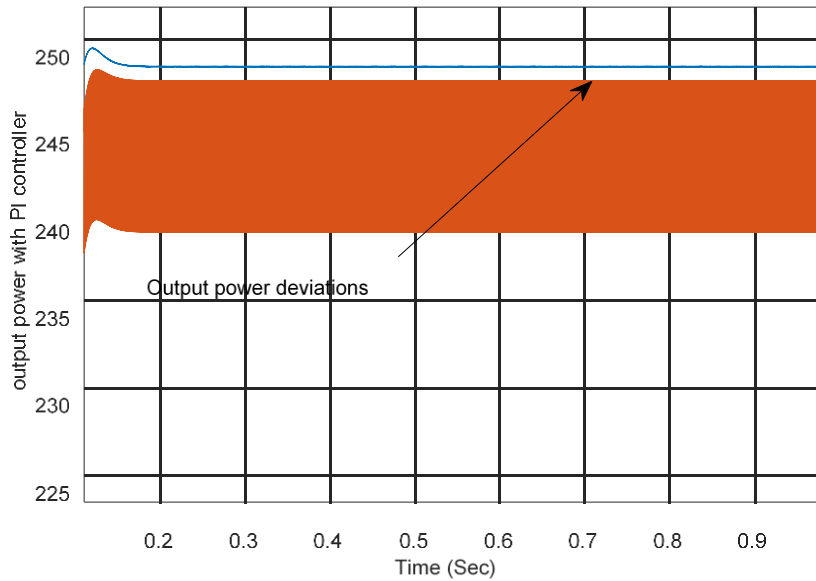


Figure 16. Output power variation with PI controller

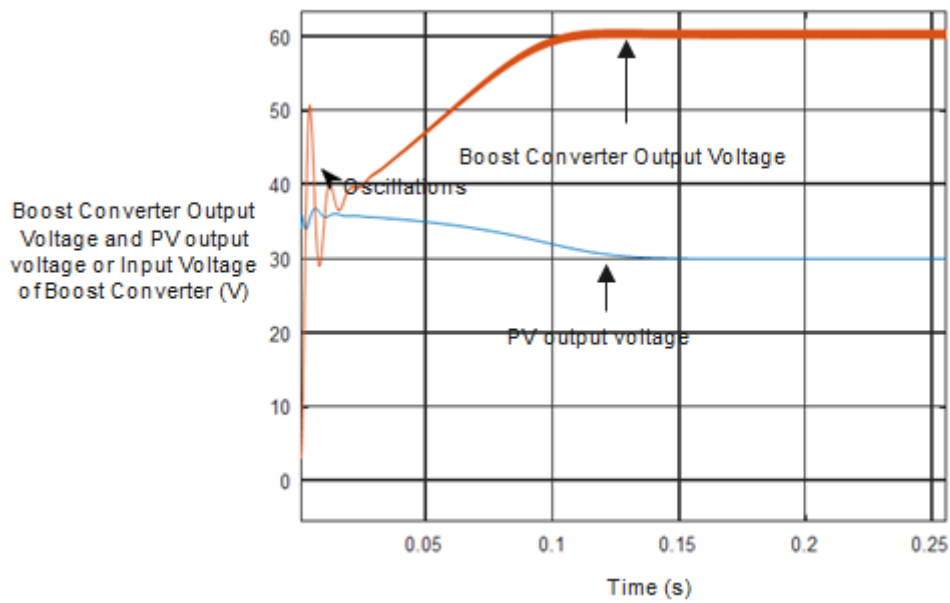


Figure 17. Output voltage of boost converter with PI controller

Output voltage of boost converter with ANN has settled time of 0.1s with negligible overshoots whereas same converter with PI control has settled time of 0.12 s and small under overshoots. Finally, time domain specification ANN has proficient than PI control for same boost converter with PV system.

VIII.CONCLUSION

One of the primary goals of the paper was to create an ANN-based MPPT controller. Various levels of irradiation were tested in the panel, and a standard voltage reference was used as a benchmark. The controllers used in this work compared the actual voltage and the reference voltage to determine the duty cycle of the boost converter. The proposed system has been shown to be superior in terms of fully utilising solar energy. ANN controllers have the potential to reduce power losses significantly. Existing MPPT methods can be significantly improved as an added benefit of using the ANN MPPT strategy. The stepping-up converter produced a constant output regardless of the amount of solar irradiation. The proposed system prototype will be built in the future.

REFERENCES

- [1] R. Ayaz, I. Nakir, and M. Tanrioven, An Improved Matlab-Simulink Model of PV Module considering Ambient Conditions, International Journal of Photoenergy, Hindawi Publisher, 2014.
- [2] Farzad Sedaghati, Ali Nahavandi, at, el. PV Maximum Power-Point Tracking by Using Artificial Neural Network, Mathematical Problems in Engineering, Hindawi publishing corporations.
- [3] S. Balakumar, B. Baskaran, "Design and Modelling of Wind Fed Resonant DC-DC Converter through Synchronous Generator using MATLAB/Simulink," International Journal of Computer Applications (0975 – 8887) Volume 73–No.3, July 2013.
- [4] Meng Zhang, Yang Li, "Deep Learning for Short-Term Voltage Stability Assessment of Power Systems, special section on key enabling technologies for prosumer energy management", IEEE Access, Vol 9, Feb, 2021.
- [5] Zhi-biao Shi at el, "Comparison of Algorithms for an Electronic Nose in Identifying Liquors", journal of bionic engineering, science direct, Vol.5, Sep.2018.
- [6] Yang Li Ph.D, at el, "Stochastic optimal scheduling of demand response-enabled microgrids with renewable generations: An analytical-heuristic approach, Journal of Cleaner Production Volume 330, 1 January 2022.
- [7] Yang Li at el, "Privacy-Preserving Spatiotemporal Scenario Generation of Renewable Energies: A Federated Deep Generative Learning Approach". IEEE transactions on industrial informatics, Pp.2310-2320, Vol.18, 20, July 2021.
- [8] <https://www.google.com/search?q=solar+radiation+in+ethiopia>.
- [9] Ashebir Dingeto Hailu and Desta Kalbessa Kumsa "Ethiopia renewable energy potentials and current state" Aims press Energy, Nov, 2020.
- [10] Abdelkhalek Chellakhi, at el, An Improved Maximum Power Point Approach for Temperature Variation in PV System Application, International Journal of Photoenergy, Hindawi publisher 2021.
- [11] J. A. Gow and C. D. Manning, "Development of a photovoltaic array model for use in power-electronics simulation studies," IEE Proceedings: Electric Power Applications, vol. 146, no. 2, pp. 193–200, 1999.